

Research Article

Viscoelastic Fluid over a Stretching Sheet with Electromagnetic Effects and Nonuniform Heat Source/Sink

Kai-Long Hsiao

Department of the Digital Technology and Applications, Diwan University, 87-1, Nansh Li, Madou Jen, Tainan 72153, Taiwan

Correspondence should be addressed to Kai-Long Hsiao, hsiao.kailong@msa.hinet.net

Received 19 October 2009; Revised 3 January 2010; Accepted 6 May 2010

Academic Editor: Kumbakonam R. Rajagopal

Copyright © 2010 Kai-Long Hsiao. This is an open access article distributed under the Creative Commons Attribution License, which permits unrestricted use, distribution, and reproduction in any medium, provided the original work is properly cited.

A magnetic hydrodynamic (MHD) of an incompressible viscoelastic fluid over a stretching sheet with electric and magnetic dissipation and nonuniform heat source/sink has been studied. The buoyant effect and the electric number E_1 couple with magnetic parameter M to represent the dominance of the electric and magnetic effects, and adding the specific item of nonuniform heat source/sink is presented in governing equations which are the main contribution of this study. The similarity transformation, the finite-difference method, Newton method, and Gauss elimination method have been used to analyze the present problem. The numerical solutions of the flow velocity distributions, temperature profiles, and the important wall unknown values of $f''(0)$ and $\theta'(0)$ have been carried out. The parameter Pr , E_1 , or E_c can increase the heat transfer effects, but the parameter M or A^* may decrease the heat transfer effects.

1. Introduction

The study of steady boundary layer flow and heat transfer of non-Newtonian fluid is relevant to several applications in the field of science and engineering. The investigation of steady boundary layer flows over a stretching surface has many important applications such as the boundary layer along a liquid film condensation process the cooling process of metallic plate in a cooling bath and in the glass of polymer industries. Some of these fluids, which can be formulated by the model used in the present study, are termed second-grade fluids. It is a well-known fact in the studies of non-Newtonian fluid flows by Hartnett [1]. Thus, if we use a non-Newtonian fluid as the coolant of the cooling systems or heat exchangers, it might greatly reduce the required pumping power. Therefore, a fundamental analysis of

the flow field of non-Newtonian fluids in a boundary layer adjacent to a stretching sheet or an extended surface is very important and is also an essential part in the area of the fluid dynamics and heat transfer. Srivastava [2] and Rajeswari and Rathna [3] studied the non-Newtonian fluid flow near a stretching sheet. Mishra and Panda [4] analyzed the behavior of second-grade viscoelastic fluids under the influence of a side-wall injection in an entrance region of a pipe flow. P. S. Gupta and A. S. Gupta [5] analyzed the viscous flow and heat transfer by an isothermal stretching sheet with suction/injection. Chen and Char [6] studied the flow and heat transfer due to a linearly stretching sheet with suction or blowing and with power law surface temperature with prescribed surface heat flux.

Rajagopal et al. [7] examined the flow field and obtained similarity solutions of the boundary layer equations numerically for the case of small viscoelastic parameter k_1 . It is shown that skin friction decreases with increase in k_1 . Dandapat and Gupta [8] examined the heat transfer problem by an exact analytical solution of the nonlinear equation governing this self-similar flow which is consistent with the numerical results in [7] given that the solutions for the temperature for various values of k_1 are presented. Later, Cortell [9] studied the heat transfer in an incompressible second-order fluid caused by a stretching sheet with a view to examine the influence of the viscoelastic parameter on that flow. In the case of fluids of differential type, the equations of motion are in general one order higher than the Navier-Stokes equations, and, in general, they need additional boundary conditions to determine the solution completely. These important issues were studied in detail by Rajagopal [10, 11] and Rajagopal and Gupta [12]. On the other hand, Subhas and Veena [13] and Subhas Abel et al. [14] investigated a viscoelastic fluid flow and heat transfer in a porous medium over a stretching sheet. However, an important finding was that the effect of viscoelasticity is to decrease the dimensionless surface temperature profiles in that flow. Later, Vajravelu and Roper [15] analyzed the effects of work due to deformation in that equation. Recently Subhas Abel et al. [16] have studied viscoelastic MHD flow and heat transfer over a stretching sheet with viscous and Ohmic dissipations; the study considers the viscous and Ohmic dissipations phenomena but does not include nonuniform heat source/sink together, so that adding to the different items are this work difference extension.

Motivated by all these studies, therefore, in the present investigation, a study for heat transfer problem has been undertaken to provide results for the MHD flow of a second-grade fluid adjacent to a stretching sheet with electric and magnetic dissipation effects and nonuniform heat source/sink for its flow field.

2. Theory and Analysis

The steady two-dimensional magneto hydrodynamic (MHD) laminar flow of an incompressible viscoelastic fluid over a thermal forming stretching sheet with electric and magnetic dissipation effects and nonuniform heat source/sink was considered. A constant magnetic field of strength parameter B_0 and electric field parameter E_1 is applied perpendicular to the thermal forming stretching sheet. Under the usual boundary layer assumptions and in the absence of pressure gradient, the steady basic boundary layer equations govern the MHD flow of viscoelastic fluid. Let us consider the steady, incompressible, two-dimensional MHD flow of a viscoelastic thin liquid film of uniform thickness over the horizontal thermal forming stretching sheet and consider the nonuniform heat source/sink q^* . The fluid motion within the film is due to stretching of the elastic sheet. The geometry of the problem is shown in Figure 1.

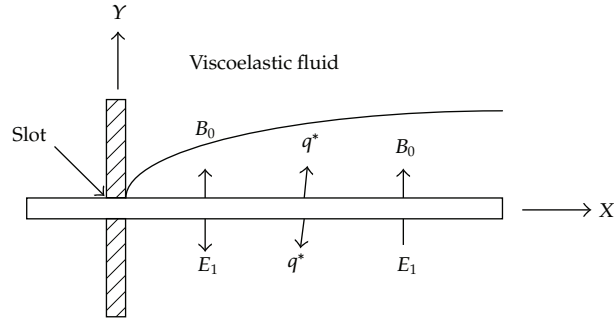


Figure 1: A sketch of the physical model for steady flow with electric and magnetic effects of an incompressible viscoelastic fluid over a thermal forming stretching sheet coupled with nonuniform heat source/sink.

An incompressible, homogeneous, non-Newtonian, second-grade fluid having a constitutive equation based on the postulate of gradually fading memory suggested by Rivlin and Ericksen [17] is used for the present flow. The model equation is expressed as follows:

$$T = -PI + \mu A_1 + \alpha_1 A_2 + \alpha_2 A_1^2, \quad (2.1)$$

where T is the stress tensor, I is the unit tensor, P is the pressure, μ is the dynamic viscosity, and α_1 and α_2 are the first and second normal stress coefficients that are related to the material modulus, and for the present second-grade fluid

$$\mu \geq 0, \quad \alpha_1 > 0, \quad \alpha_1 + \alpha_2 = 0. \quad (2.2)$$

The kinematic tensors A_1 and A_2 are defined as

$$A_1 = \nabla V + (\nabla V)^T, \quad (2.3)$$

$$A_2 = \frac{dA_1}{dt} + A_1(\nabla V) + (\nabla V)^T A_1, \quad (2.4)$$

where V is velocity, and d/dt is the material time derivative. As mentioned by Markovitz and Coleman [18], Acrivos [19], and Beard and Walters [20], this model is applicable to some dilute polymers. In the present analysis we consider the flow of a second-grade fluid obeying the steady two-dimensional boundary layer equations which for this flow, heat transfer, and mass transfer, in usual notations, are

$$\frac{\partial u}{\partial x} + \frac{\partial v}{\partial y} = 0, \quad (2.5)$$

$$u \frac{\partial u}{\partial x} + v \frac{\partial u}{\partial y} = \nu \frac{\partial^2 u}{\partial y^2} + k_1 \left[\frac{\partial}{\partial x} \left(u \frac{\partial^2 u}{\partial y^2} \right) + \frac{\partial u}{\partial y} \frac{\partial^2 u}{\partial y^2} + v \frac{\partial^3 u}{\partial y^3} \right] + \frac{\sigma E_0 B_0}{\rho} - \frac{\sigma B_0^2}{\rho} u, \quad (2.6)$$

$$\rho c_p \left(u \frac{\partial T}{\partial x} + v \frac{\partial T}{\partial y} \right) = k \frac{\partial^2 T}{\partial y^2} + \mu \left(\frac{\partial u}{\partial y} \right)^2 + (u B_0)^2 \sigma - (E_0)^2 \sigma + q^*, \quad (2.7)$$

where u, v are the velocity components in the x and y directions, $k_1 = \alpha_1 B / \mu$ is the viscoelastic parameter, ρ is the density, c_p is the specific heat at constant pressure, k is the conductivity, σ is the electrical conductivity, E_0 is the electric field factor, B_0 is the magnetic field factor, and both terms $(uB_0)^2 \sigma$ and $(E_0)^2 \sigma$ stand for the electric and magnetic dissipation. The stretching sheet was an extrusion product by this study. $q^* = (ku_w(x)/xv)[A^*(T_w - T_\infty)f'(\eta) + B^*(T - T_\infty)]$ is the space-and temperature-dependent internal heat generation/absorption. The physical mechanism about the boundary conditions is described as follows. Both u and T were assumed to be linearly dependent on x for the most simplified physical model. The sheet wall at constant temperature has the blowing and suction phenomena, and when y is large to infinite, then the velocity gradient approaches to zero and the temperature approaches to the free stream temperature. The boundary conditions to the problem are

$$\begin{aligned} u &= Bx, \quad v = v_w = -(B\nu)^{1/2} \left(m - \frac{1}{m} \right), \quad \text{at } y = 0, \\ B > 0, \quad u &\rightarrow 0, \quad \frac{\partial u}{\partial y} \rightarrow 0, \quad \text{at } y \rightarrow \infty, \\ T &= T_w = T_\infty + A \left(\frac{x}{L} \right)^2, \quad \text{at } y = 0, \\ T &\rightarrow T_\infty, \quad \text{at } y \rightarrow \infty, \end{aligned} \quad (2.8)$$

where T_w and T_∞ are constant wall temperature and ambient fluid temperature, A and B are the proportional constant, $v_w = -(B\nu)^{1/2}(m - 1/m)$, and L is the characteristic length, respectively. It should be noted that $m > 1$ corresponds to suction ($v_w < 0$) whereas $m < 1$ corresponds to blowing ($v_w > 0$). In the case when the parameter $m = 1$, the stretching sheet is impermeable. In this study, setting $m = 1$ simplified the problem in a solid wall boundary. A similarity solution for velocity will be obtained if we introduce a set of transformations, such that

$$u = Bx f'(\eta), \quad v = -(B\nu)^{1/2} f(\eta), \quad \eta = (B/\nu)^{1/2} y. \quad (2.9)$$

Equation (2.9) has satisfied the continuity equation (2.5). Substituting (2.9) into (2.6), we have

$$f'^2 - f f'' = f''' + E \left(2f' f''' - f''^2 - f f^{IV} \right) + M E_1 - M f', \quad (2.10)$$

where $E = \alpha_1 B / \mu$ is the viscoelastic parameter, $E_1 = E_0 / B_0 B x$ is the electric parameter, and $M = \sigma B_0 / \rho B$ is the magnetic parameter. L is the wall thickness of the stretching sheet. (According to a charge (q) moving with velocity u in the presence of an electric field E_0 and a magnetic field B experiences both an electric force qE_0 and a magnetic force quB . The total force, called the Lorentz force, therefore the force can be express as $F = qE_0 + quB_0$ and compare to the dimensions can be obtained $E_0 \sim uB_0$, or take it into this study $E_1 = E_0 / B_0 B x$ is a correct result, because of $u = Bx$ so that $E_1 = E_0 / B_0 u = E_0 / B_0 B x$.)

The corresponding boundary conditions become

$$\begin{aligned} f = 0, \quad f' = 1, \quad \text{at } \eta = 0, \\ f' \rightarrow 0, \quad f'' \rightarrow 0, \quad \text{at } \eta \rightarrow \infty. \end{aligned} \quad (2.11)$$

For the prescribed surface temperature, introduce the dimensionless temperature $\theta(\eta)$

$$\theta(\eta) = \frac{T - T_\infty}{T_w - T_\infty}. \quad (2.12)$$

Combining the transformations from (2.9), the energy equation becomes

$$\theta'' + \text{Pr}(f\theta' - 2f'\theta) + \text{Pr}E_c \left[(f'')^2 + M(E_1)^2 - 2E_1f' - M(f')^2 \right] + B^*\theta + A^*f' = 0, \quad (2.13)$$

where $\text{Pr} = \mu c_p / k$ is the Prandtl number and $E_c = B^2 L^2 / c_p$ is the Eckert number. A^* and B^* are parameters of space- and temperature-dependent internal heat generation/absorption. The corresponding thermal boundary conditions are

$$\begin{aligned} \theta = 1, \quad \text{at } \eta = 0, \\ \theta \rightarrow 0, \quad \text{as } \eta \rightarrow \infty. \end{aligned} \quad (2.14)$$

In terms of similarity parameters and dimensionless quantities defined by (2.9), the heating rate on the wall is

$$q_w = -k \left(\frac{\partial T}{\partial y} \right)_{y=0}. \quad (2.15)$$

Once we know the $f(\eta)$ and its derivatives, one can calculate the values of the local skin friction at the surface from the following relations:

$$\tau_x = \frac{-(\partial u / \partial y)_{y=0}}{\mu B x \sqrt{B/\nu}} = -\frac{1}{\mu} f''(0). \quad (2.16)$$

In addition, the local Nusselt number Nu_x is defined by

$$\text{Nu}_x = \frac{hx}{k} = \frac{q_w}{T_w - T_\infty} \frac{x}{k}. \quad (2.17)$$

This expression can be written as

$$\text{Nu}_x = \frac{hx}{k} = \frac{q_w}{T_w - T_\infty} \frac{x}{k} = -\theta'(0) \text{Re}^{1/2}. \quad (2.18)$$

3. Numerical Technique

In the present problem, the set of similar equations from (2.10) to (2.14) were solved by a numerical method which is combined with finite difference method, Newton's method, and Gauss elimination method. These nonlinear ordinary differential equations from (2.10) to (2.14) had been discretized by an accurate finite difference method [21], and a computer program had been developed to solve these equations. Hsiao et al. [22, 23] were also using analytical and numerical solutions to solve the related problems. In this study, we introduce the program to compute finite difference approximations of derivatives for equal spaced discrete data. The code was employed for centered differences of $O(h^2)$ for the interior points and used forward and backward differences of $O(h)$ for the first and last points, respectively. See Chapra and Canale, Numerical Methods for Engineers [24]. The finite difference formulas are divided to forward finite-difference formula for the boundary layer inner edge $\eta = 0$, backward finite-difference formula for the boundary layer outer edge $\eta = \infty$, and centered finite-difference formula for the internal points.

(1) Forward finite-difference formulas for the first derivative to fourth derivative are

$$\begin{aligned}
 f'(x_i) &= \frac{f(x_{i+1}) - f(x_i)}{h}, \\
 f''(x_i) &= \frac{f(x_{i+2}) - 2f(x_{i+1}) + f(x_i)}{h^2}, \\
 f'''(x_i) &= \frac{f(x_{i+3}) - 3f(x_{i+2}) + 3f(x_{i+1}) - f(x_i)}{h^3}, \\
 f^{(4)}(x_i) &= \frac{f(x_{i+4}) - 4f(x_{i+3}) + 6f(x_{i+2}) - 4f(x_{i+1}) + f(x_i)}{h^4}.
 \end{aligned} \tag{3.1}$$

(2) Backward finite-difference formulas for the first derivative to fourth derivative are

$$\begin{aligned}
 f'(x_i) &= \frac{f(x_i) - f(x_{i-1})}{h}, \\
 f''(x_i) &= \frac{f(x_i) - 2f(x_{i-1}) + f(x_{i-2})}{h^2}, \\
 f'''(x_i) &= \frac{f(x_i) - 3f(x_{i-1}) + 3f(x_{i-2}) - f(x_{i-3})}{h^3}, \\
 f^{(4)}(x_i) &= \frac{f(x_i) - 4f(x_{i-1}) + 6f(x_{i-2}) - 4f(x_{i-3}) + f(x_{i-4})}{h^4}.
 \end{aligned} \tag{3.2}$$

(3) Centered finite-difference formulas for first derivative to fourth derivative are

$$\begin{aligned}
 f'(x_i) &= \frac{f(x_{i+1}) - f(x_{i-1}))}{2h}, \\
 f''(x_i) &= \frac{f(x_{i+1}) - 2f(x_i) + f(x_{i-1}))}{h^2}, \\
 f'''(x_i) &= \frac{f(x_{i+2}) - 2f(x_{i+1}) + 2f(x_{i-1}) - f(x_{i-2}))}{2h^3}, \\
 f^{(4)}(x_i) &= \frac{f(x_{i+2}) - 4f(x_{i+1}) + 6f(x_i) - 4f(x_{i-1}) + f(x_{i-2}))}{h^4}.
 \end{aligned} \tag{3.3}$$

The present finite-difference method is similar to Box method [21], but it directly applies the above finite-difference formulas into the similarity boundary layer equations and solves them by using the Gauss elimination method with Newton's method [24].

The numerical study by this work includes three important parts which are named Newton's method, Gaussian elimination and finite-difference formulas. It is important because it has a satisfactory theory of existence of solutions, as well as uniqueness and continuous dependence with respect to the initial data and it explains that the initial data must be confined at some conditions.

(1) Newton's Method Restrict Conditions

- (a) Newton's method iteratively uses tangential lines that pass through the consecutive approximations for the root.
- (b) The method needs a good initial guess. Otherwise the iterative solution may diverge or converge to an irrelevant solution.

(2) Gauss Elimination Method Necessary Conditions

- (a) The number of equations must equal that of the unknowns.
- (b) Each equation is linearly independent.

To ensure the convergence of the numerical solution to exact solution, the step sizes $\Delta\eta$ have been optimized and the results presented in which are independent of the step sizes at least up to the fourth decimal place. The convergence criteria were based on the relative difference between the current and previous iteration values of the velocity and temperature gradients at wall. When the difference reaches less than 10^{-6} for the flow fields, the solution is assumed to convergence, and the iterative process is terminated.

4. Results and Discussion

The effects of dimensionless parameters are analyzed by utilizing the boundary layer concept to obtain a set of coupled momentum equation and energy equation. A similarity transformation has been used to convert the nonlinear, coupled partial differential equations to a set of nonlinear, coupled ordinary differential equations. A generalized derivation to analyze a stretching sheet flow field has been studied. An accurate numerical method

Table 1: Values of $-f''(0)$, $-\theta'(0)$ for different values of physical parameters $E = 0.001$, $Pr = 1$ and various parameters E_c , E_1 , A^* , B^* , and M .

| A^* | B^* | M | E_c | E_1 | $-f''(0)$ | $-\theta'(0)$ |
|-------|-------|-----|-------|-------|-----------|---------------|
| 0.1 | 0.1 | 0.0 | 0.1 | 0.1 | 0.0874 | 1.5301 |
| 0.2 | 0.2 | 0.1 | 0.2 | 0.1 | 0.1526 | 1.4919 |
| 0.3 | 0.3 | 0.2 | 0.3 | 0.1 | 0.2197 | 1.5051 |
| 0.4 | 0.4 | 0.3 | 0.4 | 0.1 | 0.2983 | 1.5800 |
| 0.5 | 0.5 | 0.4 | 0.5 | 0.2 | 0.3919 | 1.7195 |
| 0.6 | 0.6 | 0.5 | 0.6 | 0.2 | 0.1054 | 1.4822 |
| 0.7 | 0.7 | 0.6 | 0.7 | 0.2 | 0.0970 | 1.5673 |
| 0.8 | 0.8 | 0.7 | 0.8 | 0.2 | 0.0750 | 1.6627 |

combined with finite difference method, Newton's method, and Gauss elimination method has been used to obtain solutions of these equations. Table 1 shows the different values of skin friction $-f''(0)$ and Nusselt number $-\theta'(0)$ for different values of physical parameters.

Figure 2 depicts dimensionless velocity profiles f versus η as $E_1 = 0.1$, $E = 0.001$, and $M = 1.0, 3.0, 5.0, 10, 20$. The dimensionless velocity profiles f are satisfied by the boundary conditions and vary by a smooth curve for different M values. When the M is larger the f curve is lower, so that the momentum effect is lower for a larger M . Figures 2 and 3 show that velocity/temperature values decrease/increase as M increases, the reason is that the parameter M is standing as a magnetic force in the fluids and it may reduce the velocity/temperature values from the flow field. On the physical aspect, when the M increases, the flow will slow down and the temperature will be lower too. On the mathematical aspect, it has used a negative sign to this item on the momentum and energy equations. Figure 4 depicts dimensionless temperature profiles θ versus η as $Pr = 1$, $M = 0.1$, $A^* = 0.1$, $B^* = 0.1$, $E_c = 0.1$, $E = 0.001$ and $E_1 = 0.5, 1.5, 2.5, 3.5, 5$. The dimensionless temperature profiles θ are satisfied the boundary conditions and varies by a smooth cure for different E_1 values. When the E_1 is larger and the θ curve is lower, so that the heat transfer effect is larger for a larger E_1 . Figure 5 depicts dimensionless temperature profiles θ versus η as $Pr = 1$, $E_1 = 0.1$, $M = 0.1$, $A^* = 0.1$, $B^* = 0.1$, $E = 0.001$, and $E_c = 0.4, 0.8, 1.5, 2.5, 3.5$. The dimensionless temperature profiles θ are satisfied by the boundary conditions and vary by a smooth cure for different E_c values. When the E_c is larger the curve θ is lower, so that the heat transfer effect is higher for a larger E_c .

Figure 6 depicts dimensionless temperature profiles θ versus η as $E_1 = 0.1$, $M = 0.1$, $A^* = 0.1$, $B^* = 0.1$, $E_c = 0.1$, $E = 0.001$, and $Pr = 0.5, 1.5, 2.5, 3.5, 5.0$. The dimensionless temperature profiles θ are satisfied by the boundary conditions and vary by a smooth cure for different Pr values. When the Pr is larger the θ curve is lower, so that the heat transfer effect is larger for a larger Pr . Figure 7 depicts dimensionless temperature profiles θ versus η as $E_1 = 0.1$, $M = 0.1$, $Pr = 1$, $B^* = 0.1$, $E_c = 0.1$, $E = 0.001$, and $A^* = 0.2, 0.5, 0.8, 1.1, 1.5$. The dimensionless temperature profiles θ are satisfied the boundary conditions and vary by a smooth cure for different A^* values. When the A^* is larger the θ curve is higher, so that the heat transfer effect is lower for a larger A^* . Figure 8 depicts dimensionless temperature profiles θ versus η as $E_1 = 0.1$, $M = 0.1$, $Pr = 1$, $A^* = 0.1$, $E_c = 0.1$, $E = 0.001$, and $B^* = 0.2, 0.5, 0.8, 1.1, 1.5$. The dimensionless temperature profiles θ are satisfied by the boundary conditions and vary by a smooth cure for different B^* values. When the B^* is larger the θ curve is lower as η is less then 3; the heat transfer effect is larger for a larger B^* . On the other hand, when the B^* is larger, the θ curve is higher as η is greater than 3; the heat transfer effect

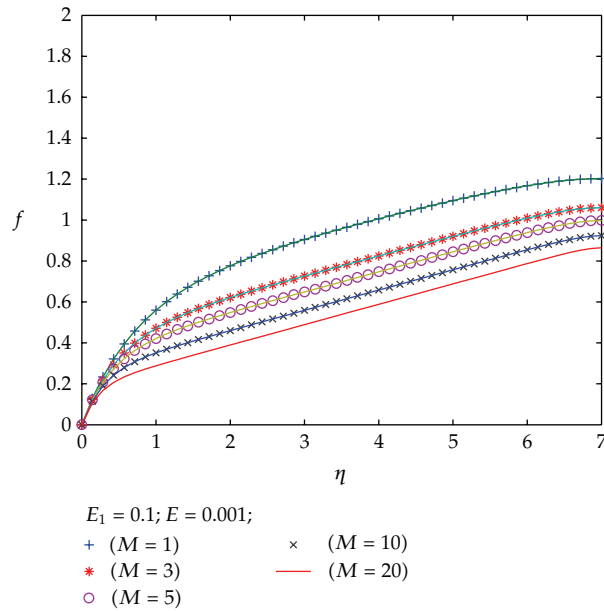


Figure 2: f versus η for various parameters.

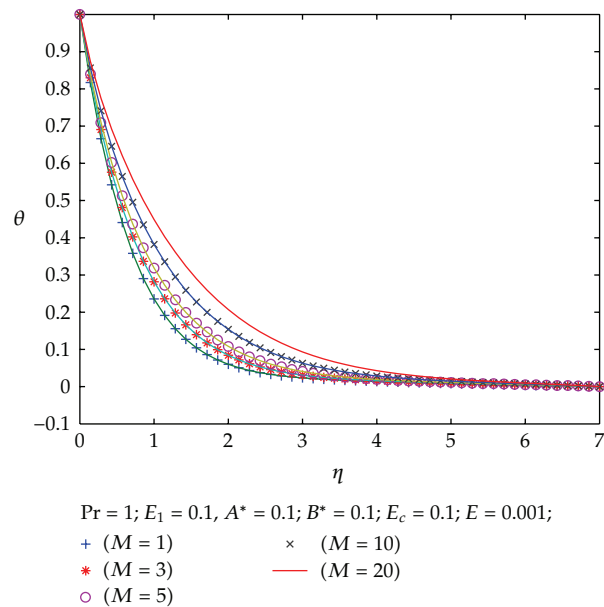


Figure 3: θ versus η for various parameters.

is lower for a larger B^* . Figures 3–8 depict dimensionless temperature gradient profiles θ' versus η . The figures show that $-\theta'(0)$ is an important factor for $-\theta'$ at $\eta = 0$ and $-\theta'(0)$ is larger when the parameter Pr , E_c , or E_1 is larger too, so that the heat transfer effect is higher at a larger parameter Pr , E_c , or E_1 . On the contrary, the parameter M or A^* is larger, the heat transfer effect is lower at a larger parameter M or A^* .

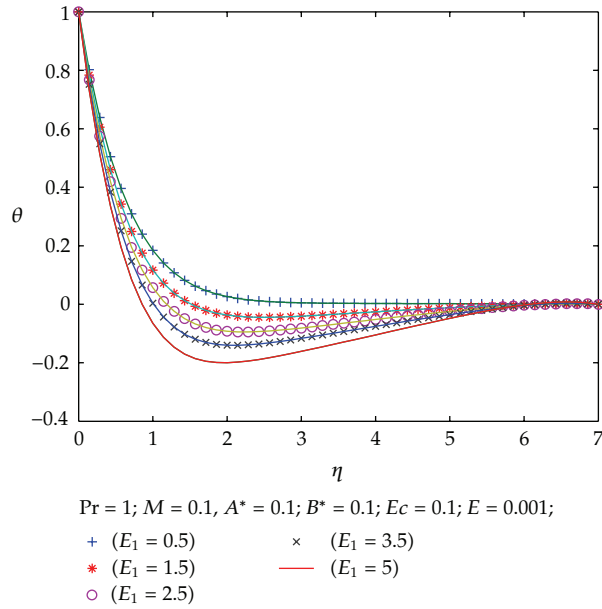


Figure 4: θ versus η for various parameters.

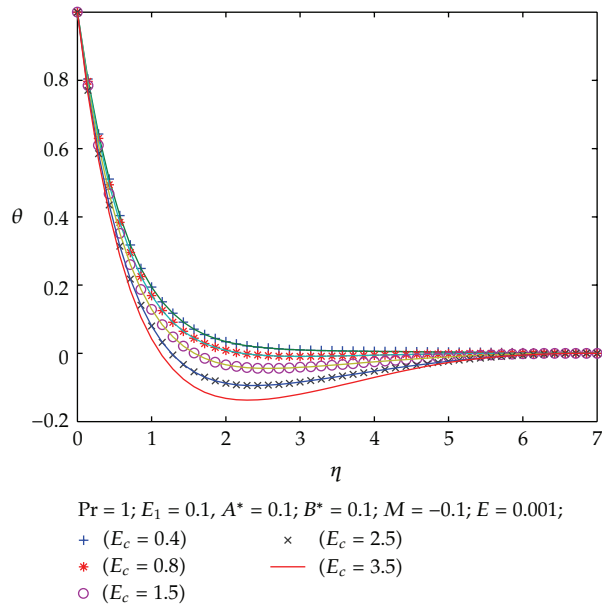


Figure 5: θ versus η for various parameters.

Figure 8 shows a special phenomenon at the $\eta \rightarrow 3$, in which the heat transfer curve appears as adverse point; this is a special highly nonlinear phenomenon in this study. In my opinion, it is a special result for this study and it is a complex influence result for different parameters.

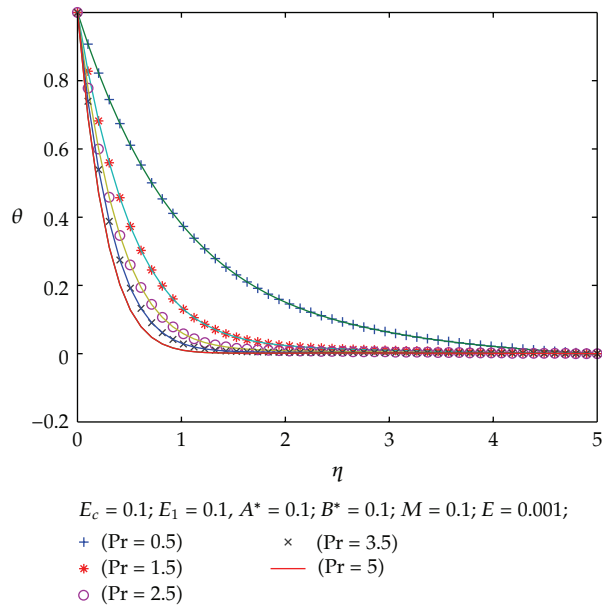


Figure 6: θ versus η for various parameters.

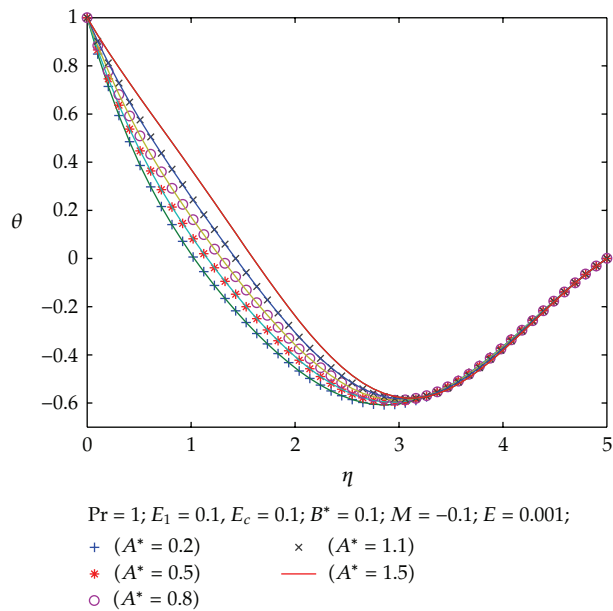


Figure 7: θ versus η for various parameters.

5. Conclusions

A heat transfer with electric and magnetic (electromagnetic) effects and with nonuniform heat source/sink for a steady two-dimensional incompressible second-grade fluid adjacent to a stretching sheet has been studied. The governing equations are solved by the similarity

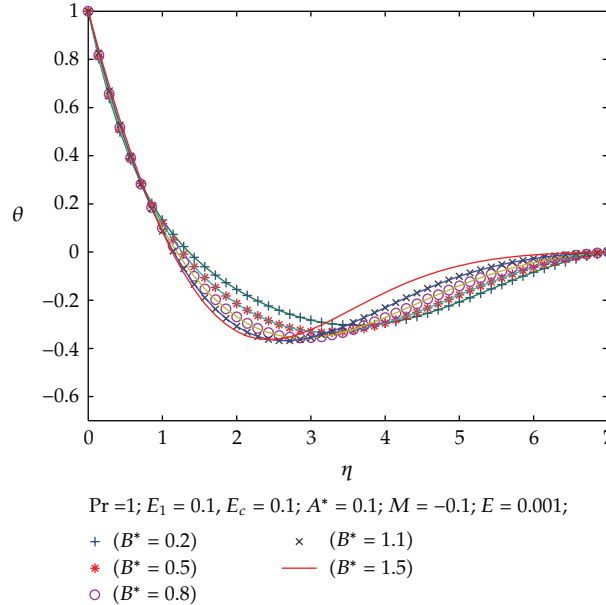


Figure 8: θ versus η for various parameters.

transformation method, finite-difference method, Gauss elimination method, Newton's method, and so forth. Dimensionless heat transfer important factor $-\theta'(0)$ increases with increasing values of E_c , Pr, and E_1 , so that the values of E_c , Pr, and E_1 are important factors in this study. It will produce greater heat transfer effect with a larger value of those parameters, but parameters M , A^* will reduce heat transfer effect. On the other hand, the high nonlinear phenomena are appearing to this study from the results of Figure 8 for parameter B^* .

- (1) It has found that from Figure 2, when magnetic parameter M increased, the dimensionless fluid velocity decreased. However the effect of momentum in the boundary layer is observed, which causes the momentum to decrease, which results in decreasing the fluid velocity. It has also been found that, from Figure 3, when the magnetic parameter M is larger, the heat transfer effect is lower at a larger magnetic parameter.
- (2) On the contrary, Figures 4–6 reveal that the increase of E_c , Pr, and E_1 results in the decrease of temperature gradient on the wall and lets $\theta'(0)$ be lower. This is because there would be a decrease of the thermal boundary layer thickness with the increase of values of E_c , Pr, and E_1 . The heat transfer phenomenon is good at these physical conditions.
- (3) It has been found that, from Figures 7 and 8, the effects of A^* and B^* are parameters of space- and temperature-dependent internal heat generation/absorption. The parameter A^* on heat transfer process may show that the increase of value of A^* results in the increase of heat transfer distribution as a result of increase of the thermal boundary layer thickness with the decreased values of A^* . Figure 8 shows a special phenomenon at the $\eta \rightarrow 3$, in which the heat transfer curve appears as adverse point, this is a special highly nonlinear phenomenon in this study.

- (4) The features in this study are combined with many parameter effects (M , Pr , E_1 , A^* , B^* , and E_c) for a non-Newtonian viscoelastic second-grade fluid heat transfer problem and solved it by a specific numerical method which is different from the other similar works.

Acknowledgments

The author would like to thank the valuable comments which were provided by the reviewers and would like to thank Professor K. R. Rajagopal for his editorial helping. On the other hand, He would like to thank National Science Council China for the financial support through Grant NSC 98-2221-E-434-009.

References

- [1] J. P. Hartnett, "Viscoelastic fluids. A new challenge in heat transfer," *Journal of Heat Transfer*, vol. 114, no. 2, pp. 296–303, 1992.
- [2] A. C. Srivastava, "The flow of a non-Newtonian liquid near a stagnation point," *Zeitschrift für angewandte Mathematik und Physik ZAMP*, vol. 9, no. 1, pp. 80–84, 1958.
- [3] G. K. Rajeswari and S. L. Rathna, "Flow of a particular class of non-Newtonian visco-elastic and visco-inelastic fluids near a stagnation point," *Zeitschrift für Angewandte Mathematik und Physik*, vol. 13, pp. 43–57, 1962.
- [4] S. P. Mishra and T. C. Panda, "Effect of injection on the flow of second order fluid in the inlet region of a channel," *Acta Mechanica*, vol. 32, no. 1–3, pp. 11–17, 1979.
- [5] P. S. Gupta and A. S. Gupta, "Heat and mass transfer on a stretching sheet with suction or blowing," *The Canadian Journal of Chemical Engineering*, vol. 55, pp. 744–746, 1977.
- [6] C. K. Chen and M. I. Char, "Heat transfer of a continuous, stretching surface with suction or blowing," *Journal of Mathematical Analysis and Applications*, vol. 135, no. 2, pp. 568–580, 1988.
- [7] K. R. Rajagopal, T. Y. Na, and A. S. Gupta, "Flow of a viscoelastic fluid over a stretching sheet," *Rheologica Acta*, vol. 23, no. 2, pp. 213–215, 1984.
- [8] B. S. Dandapat and A. S. Gupta, "Flow and heat transfer in a viscoelastic fluid over a stretching sheet," *International Journal of Non-Linear Mechanics*, vol. 24, no. 3, pp. 215–219, 1989.
- [9] R. Cortell, "Similarity solutions for flow and heat transfer of a viscoelastic fluid over a stretching sheet," *International Journal of Non-Linear Mechanics*, vol. 29, no. 2, pp. 155–161, 1994.
- [10] K. R. Rajagopal, "On boundary conditions for fluids of the differential type," in *Navier-Stokes Equations and Related Nonlinear Problems*, pp. 273–278, Plenum Press, New York, 1995.
- [11] K. R. Rajagopal, "On the creeping flow of the second-order fluid," *Journal of Non-Newtonian Fluid Mechanics*, vol. 15, no. 2, pp. 239–246, 1984.
- [12] K. R. Rajagopal and A. S. Gupta, "An exact solution for the flow of a non-Newtonian fluid past an infinite porous plate," *Meccanica*, vol. 19, no. 2, pp. 158–160, 1984.
- [13] A. Subhas and P. Veena, "Visco-elastic fluid flow and heat transfer in a porous medium over a stretching sheet," *International Journal of Non-Linear Mechanics*, vol. 33, no. 3, pp. 531–540, 1998.
- [14] M. Subhas Abel, A. Joshi, and R. M. Sonth, "Heat transfer in MHD visco-elastic fluid flow over a stretching surface," *ZAMM Zeitschrift für Angewandte Mathematik und Mechanik*, vol. 81, no. 10, pp. 691–698, 2001.
- [15] K. Vajravelu and T. Roper, "Flow and heat transfer in a second grade fluid over a stretching sheet," *International Journal of Non-Linear Mechanics*, vol. 34, no. 6, pp. 1031–1036, 1999.
- [16] M. Subhas Abel, E. Sanjayanand, and M. M. Nandeppanavar, "Viscoelastic MHD flow and heat transfer over a stretching sheet with viscous and ohmic dissipations," *Communications in Nonlinear Science and Numerical Simulation*, vol. 13, no. 9, pp. 1808–1821, 2008.
- [17] R. S. Rivlin and J. L. Ericksen, "Stress-deformation relations for isotropic materials," *Journal of Rational Mechanics and Analysis*, vol. 4, pp. 323–425, 1955.
- [18] H. Markovitz and B. D. Coleman, "Incompressible second-order fluids," in *Advances in Applied Mechanics*, Vol. 8, pp. 69–101, Academic Press, New York, NY, USA, 1964.

- [19] A. Acrivos, "A theoretical analysis of laminar natural convection heat transfer to non-Newtonian fluids," *AIChE Journal*, vol. 6, no. 4, pp. 584–590, 1960.
- [20] D. W. Beard and K. Walters, "Elastico-viscous boundary-layer flows. I. Two-dimensional flow near a stagnation point," *Proceedings of the Cambridge Philosophical Society*, vol. 60, pp. 667–674, 1964.
- [21] T. Cebeci and P. Bradshaw, *Physical and Computational Aspects of Convective Heat Transfer*, Springer, New York, NY, USA, 1984.
- [22] K.-L. Hsiao and G.-B. Chen, "Conjugate heat transfer of mixed convection for viscoelastic fluid past a stretching sheet," *Mathematical Problems in Engineering*, vol. 2007, Article ID 17058, 21 pages, 2007.
- [23] K.-L. Hsiao, "Conjugate heat transfer of magnetic mixed convection with radiative and viscous dissipation effects for second-grade viscoelastic fluid past a stretching sheet," *Applied Thermal Engineering*, vol. 27, no. 11-12, pp. 1895–1903, 2007.
- [24] S. C. Chapra and R. Canale, *Numerical Methods for Engineers*, McGraw-Hill, New York, NY, USA, 2nd edition, 1990.